JOC The Journal of Organic Chemistry

ARTICLE

pubs.acs.org/joc

Mechanism of the Pechmann Reaction: A Theoretical Study

János Daru[†] and András Stirling[*,‡]

[†]Eötvös Loránd University, Budapest, Hungary

[‡]Chemical Research Center of Hungarian Academy of Sciences, Budapest, Hungary

Supporting Information

ABSTRACT: One of the most widespread synthetic routes to coumarins is the condensation of esters and phenols via the Pechmann reaction. Despite the industrial and technological importance of the reaction, its mechanism is still poorly understood. We have explored several possible reaction paths by DFT calculations at the M05−2X/6-31+G* level. Amphoteric groups and the solvent have a crucial role in the frequent proton-transfer steps of the mechanisms; therefore, we have employed a mixed solvent model, where we combined the implicit PCM model together with an explicit water molecule placed at the actual proton transfer region. The Gibbs free-energy profiles of the possible routes suggest that three parallel channels (featuring water elimination, trans-esterification, and electrophilic attack) operate simultaneously. Enolic routes have prohibitively high activation barriers rendering these paths untenable. The calculated profiles indicate that in each feasible route the first elementary step has the highest activation energy. Reaction intermediates identified on the free-energy profiles can explain several experimental observations.

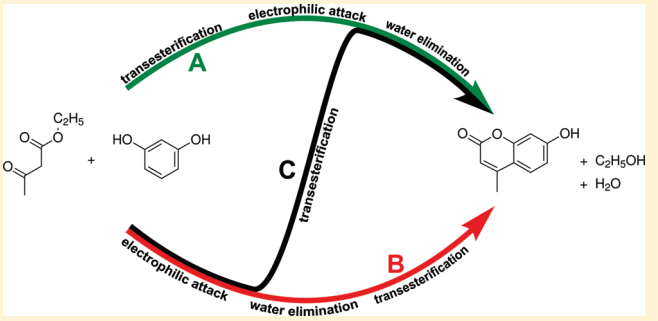

1. INTRODUCTION

Coumarin and its derivatives are widely occurring natural compounds in plants, in micro-organisms, and in animals.[1−3] Since their first isolation in the 1820s, they have been obtained from over 800 plant species and more than 1000 derivatives have been investigated.[4] Coumarins have recently gained increasing importance due to their technological potential in pharmaceutical, agrochemical and fragrance industries. For instance, coumarin derivatives show remarkable activities in various medical problems (HIV, blood coagulation, tumors, infections, inflammations),[2,3,5] many of them have favorable antioxidant and antimicrobial effects and enzyme inhibition properties.[3−6] Besides their biological activity, coumarin derivatives are also widely applied in food and cosmetic industry[7] and in color technology as optical brightening agents or laser dyes.[1,4,8]

One of the possible synthetic routes for coumarins is the condensation reaction by Hans von Pechmann.[9] In the Pechmann reaction (Figure 1), activated phenols and ethyl acetoacetate yield coumarins and the byproducts ethanol and water.

Since the reactants are cheap and easily available, this process is the most widely applied synthetic route for coumarins.[8,10,11] The original reaction is conducted at elevated temperature. As it employs strongly acidic conditions, the reaction produces harmful, acidic wastewater. In addition, the harsh conditions imply limitations on the possible reactants or necessitate the application of protective groups. Various improvements have been suggested employing either Brønsted-acids (free, or solid-supported): HCl, HCl/CH_3COOH, HCl/CH_3CH_2OH, H_3PO_4,[12] $HClO_4$,[13]

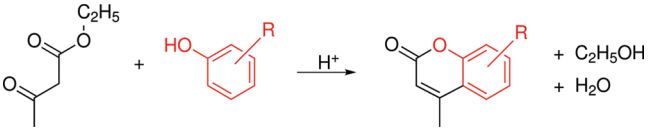

Figure 1. Pechmann reaction.

CF_3COOH,[14] CF_3SO_3H,[15] $(COOH)_2$,[16] heteropoly acids,[17] aqueous solution of ionic-liquids,[18] ion-exchange resins[19] as well as Lewis acids, such as $AlCl_3$, $ZnCl_2$[12] or $InCl_3$.[20]

Despite the importance of coumarins and the technological significance of their production, the underlying mechanism is poorly understood. Two different mechanisms have been put forward earlier[12,21] which have been later adapted albeit often with minor modifications. The mechanism proposed by Robertson et al. (Figure 2) starts with an electrophilic attack by the β-carbonyl group of the ethyl acetoacetate to the aromatic ring. They supported their proposal by isolating cinnamic acid as an intermediate, and they could convert cinnamic acid derivatives to coumarins.[12,21] Recently another intermediate (2,4-dihydroxy-ethyl-trans-β-methylcinnamate) has also been observed, supporting this sequence.[22]

The proposal by Ahmed and Desai (Figure 3) features the esterification as the first step, followed by the electrophilic attack for ring closure.[12] Their mechanism can also account for the

Received: July 12, 2011
Published: September 20, 2011

   dx.doi.org/10.1021/jo201439u | J. Org. Chem. 2011, 76, 8749–8755

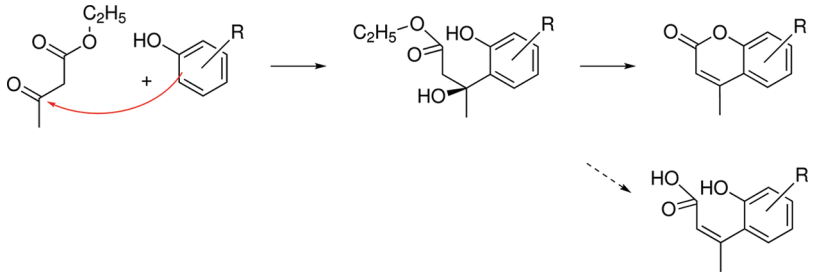

Figure 2. Mechanism proposed by Robertson at al. The lower route indicates the proposed side-reaction.

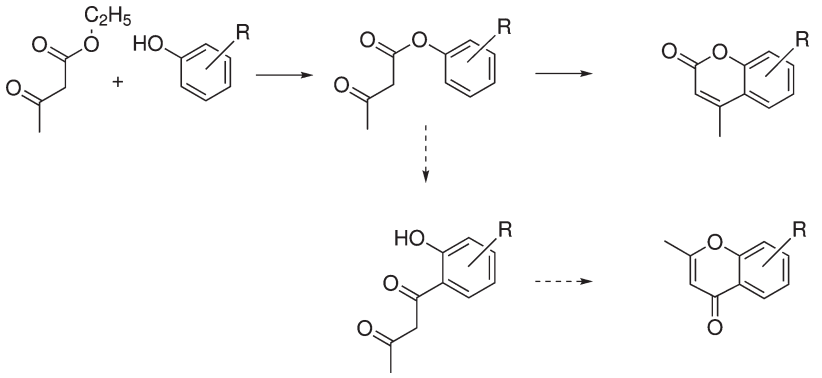

Figure 3. Mechanism proposed by Ahmed and Desai. The lower route indicates the proposed side-reaction.

formation of chromone side-product, by assuming that Fries-migration can take place after the esterification step.

Both proposals have been often claimed to be "the mechanism of the reaction" in literature. Some papers prefer the mechanistic proposal by Robertson et al,[14] others have referred to the mechanism of Ahmed and Desai,[14,17,19,23] while there are also a few papers invoking both.[12,24] A further complication in the mechanistic views is whether the electrophilic attack occurs via the oxo[12,14,17,23,24] or the enol form[19,23,25] of the β-keto-aryl ester. This issue has not been resolved either.

Clearly, a detailed experimental investigation of the mechanism and in particular the kinetics has been hampered by the conditions usually employed for the Pechmann condensations, although recently promising results have been obtained using in situ Raman technology.[23] Therefore to obtain detailed insight into the Pechmann reactions and to identify the most likely reaction routes we have performed density functional calculations. Curiously, to the best of our knowledge this is the first study aimed at investigating the Pechmann mechanism theoretically. We have selected the 7-hydroxy-4-methylcoumarin as a typical and technologically relevant product of the Pechmann condensation to study. We have calculated the full free energy profiles of the possible reaction channels. Our main motivations are to identify the feasible reaction paths, to select intermediates that can be promising candidates for experimental detection and to provide a detailed mechanistic picture of the process that may then help to develop more effective and environmentally benign versions of the Pechmann reaction.

2. COMPUTATIONAL DETAILS

The calculations have been carried out at the M05−2X/6-31+G* level, applying ultrafine grid with the Gaussian 09 package.[26] The basis set convergence has been verified by comparing the results obtained with the 6-31G*, 6-31+G*, and 6-311+G* basis sets. The functional applied in this study has been shown to provide accurate geometries, thermochemistry and kinetics.[27] The methodology has been tested against MP2/6-311++G** for the full B path. The mean unsigned energy difference between the successive structures of the mechanism was 1.1 kcal/mol while the largest discrepancy was 2.6 kcal/mol. The basis set superposition error has been estimated to be around 2 kcal/mol. All stable molecules and transition state (TS) structures have been verified by vibrational analysis. Additional IRC and normal optimization calculations always showed that the calculated TS-s connect the two minima characterizing the elementary step in question. Solvent effects have been taken into account by employing a mixed solvent model: we have applied an explicit, strategically placed water molecule to enhance proton transfers, and the SMD implicit continuum solvation model.[28] The SMD method for cations has an average error of 3.1 kcal/mol;[28] hence, we consider this as the main source of error in our methodology. As solvent models for the most important acids were not available in Gaussian 09, we have employed the water parametrization. In addition, we do not take into account the temperature dependence of the parametrization. Although the present solvation model is not rigorously complete, we expect that solvation effects are treated sufficiently to distinguish between the mechanisms. The Gibbs free energy contributions to the electronic energy contribution have been calculated employing the harmonic oscillator, rigid rotor, ideal gas approximation at 110 °C and 1 mol/dm^3, and including the solvation free energy changes. Note that for some of the elementary steps we had to alter the position of the explicit water molecule to properly describe the subsequent step and the two configurations necessarily have different energies (2−4 kcal/mol). In such cases, we give the deeper level on the free energy diagrams.

3. RESULTS AND DISCUSSION

The starting point of our investigation is a retrosynthetic analysis of the Pechmann reaction, which revealed three essential transformations constituting the pathways: water elimination,

dx.doi.org/10.1021/jo201439u |J. Org. Chem. 2011, 76, 8749–8755

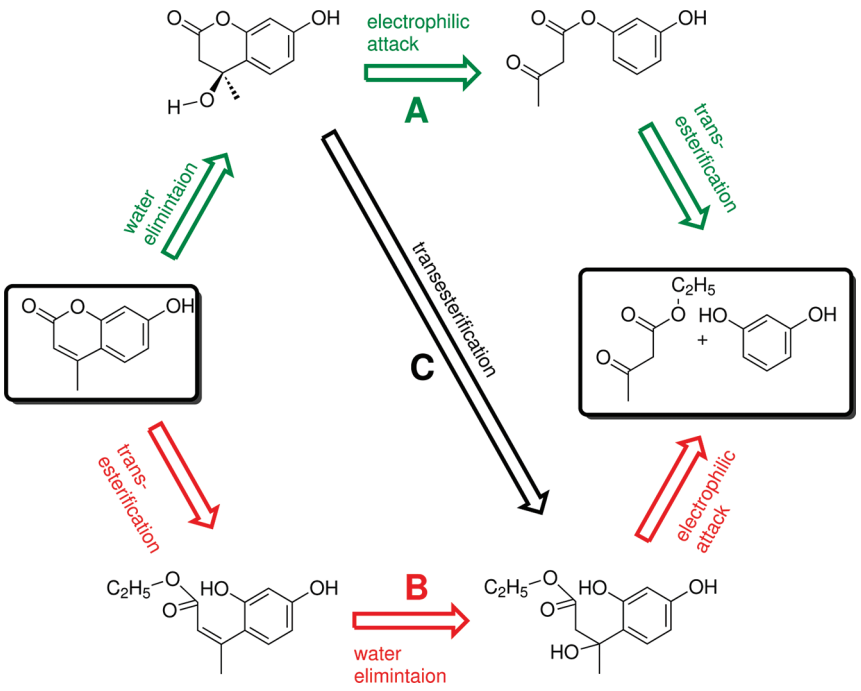

Figure 4. Retrosynthetic analysis of coumarin.

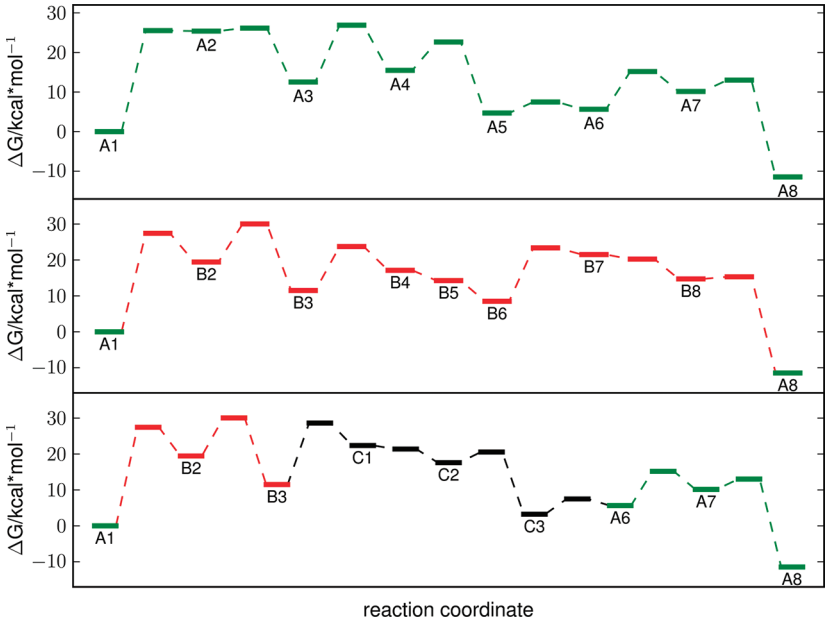

Figure 5. Gibbs free energy diagram for "A" mechanism (upper panel), "B" mechanism (middle panel) and "C" mechanism (lower panel).

trans-esterification and an electrophilic attack of the acetyl group. Since electrophilic attack has to precede water elimination, the possible six different combinations of these steps can be reduced to three possible reaction sequences (see Figure 4):

A) trans-esterification; electrophilic attack; water elimination
B) electrophilic attack; water elimination; trans-esterification
C) electrophilic attack; trans-esterification; water elimination

The reaction routes also involve various conformational changes, which we have explored in detail. Nevertheless, on the free energy profiles (Figure 5), we have plotted only those that have activation barrier higher than 5 kcal/mol.

3.1. Oxo Routes. The free energy profiles calculated for the A, B and C oxo routes are displayed in Figure 5. The corresponding reaction schemes with the most important stationary structures can be seen on Figures 6−8. We note that all free energy profiles are referenced to A1. The initial configuration of routes B and C (B1) is 6.9 kcal/mol higher in energy and can be reached from A1 via simple proton transfer. Inspection of the diagrams reveals common motifs. The most striking feature of the profiles is that the first step of each route requires the highest activation free energy. The stoichiometry of the Pechmann reaction suggests bimolecular mechanism, although stoichiometry and molecularity

dx.doi.org/10.1021/jo201439u |J. Org. Chem. 2011, 76, 8749–8755

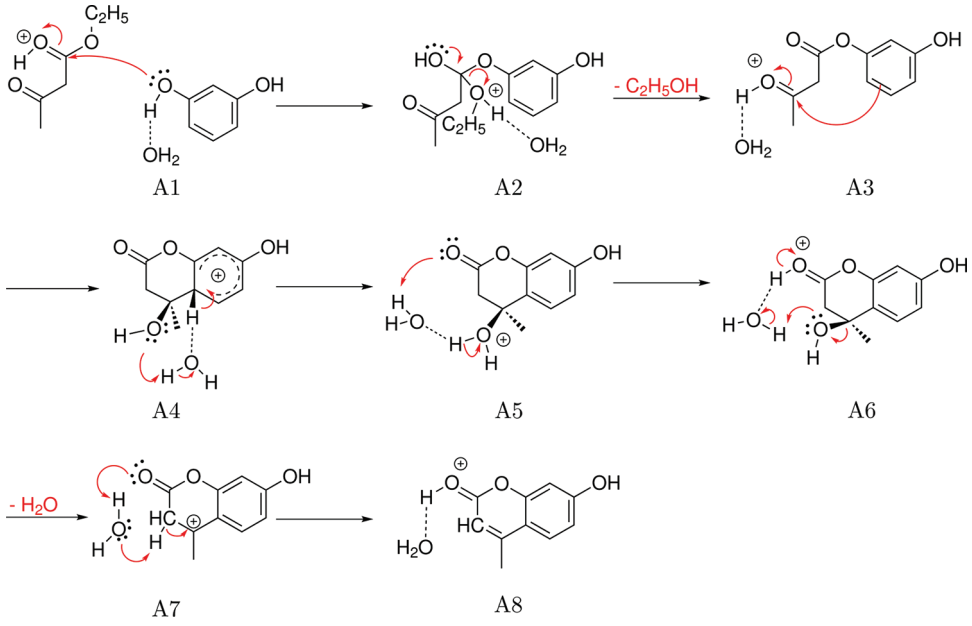

Figure 6. Reaction scheme of the "A" mechanism.

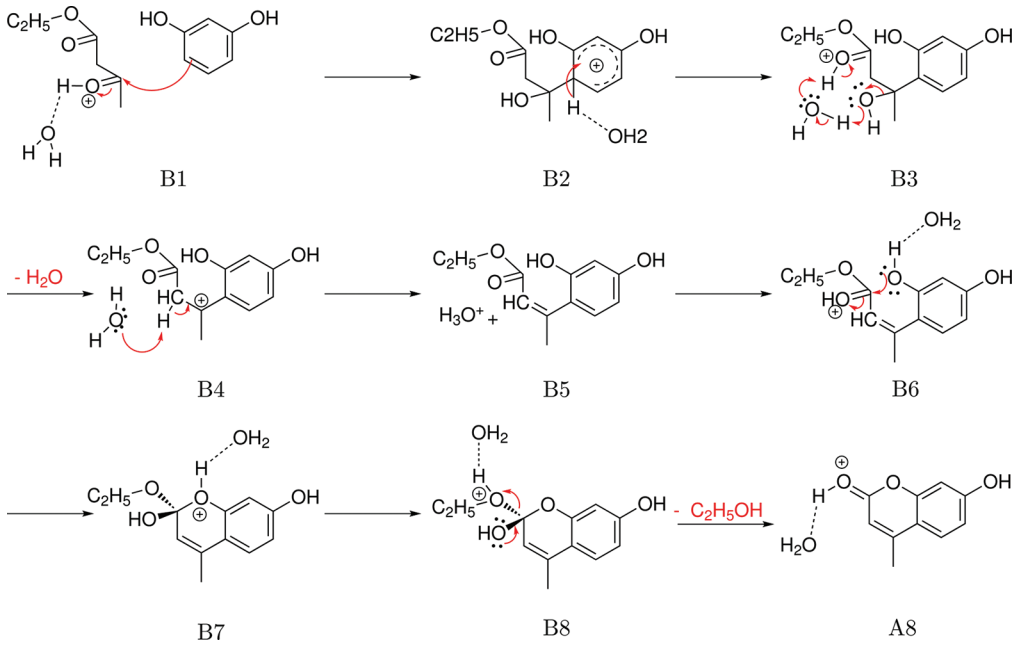

Figure 7. Reaction scheme of the "B" mechanism.

are not directly related. Indeed, the reaction schemes show that all routes start with the association of the two reactants. Hence, the large energy differences seen at the beginning of each path are partly due to the entropy loss associated with the bimolecular-unimolecular transformation. In the gas-phase, this entropy contribution can amount to 10−14 kcal/mol;[29] hence, a dominant part of the activation energy for the Pechmann reaction can be explained by the bimolecularity of the mechanism. The next steps forward can be considered unimolecular reactions. It is important to note that the trans-esterification and water elimination yield byproducts, that is, the number of molecules increases at these steps. Hence, they give rise to entropy gains, which contribute significantly to the overall exergonicity of the Pechmann reaction (−11.4 kcal/mol). An important experimental observation is that the Pechmann condensation is exergonic, but not spontaneous in short time-scales (i.e., does not take place in measurable amounts at ambient temperature). In fact, it requires initialization, and various energy sources have been employed. Besides the most frequent thermal induction, ultrasound[30] and microwave irradiations[25] have also proved to be very efficient. We conclude therefore that our calculations are in agreement with the experimental observations indicating a reasonable barrier and exergonicity for the Pechmann condensation.

dx.doi.org/10.1021/jo201439u |J. Org. Chem. 2011, 76, 8749–8755

Another important aspect of the reaction paths is the frequent proton transfer emerged from the calculations. This is in agreement with the acid catalysis but poses a technical problem: the migrating proton represents a concentrated charge region that cannot be sufficiently stabilized by the implicit solvent techniques. Introducing a single explicit water molecule at the close vicinity of the proton transfer region has a 2-fold role: it catalyzes the proton migration via H-bond relay and screens the proton charge efficiently. Similar combined explicit−implicit approaches have been already suggested and applied successfully.[31] As our calculated mechanisms show, the explicite water molecule plays an important role in several steps and the corresponding activation energies associated with these proton migrations are always small (1−10 kcal/mol).

Intermediates that can transform with relatively high activation energy in either the forward or backward directions can be candidates for experimental detection. All of the paths feature such structures, namely A3 on route A, B3 and B6 on route B, and B3 on route C. The higher activation energies resulting in the stability of these intermediates correspond to C−C, C−O bond formations and aromatizations. In contrast, the acid−base steps are always faster and produce more reactive intermediates having presumably very short lifetime.

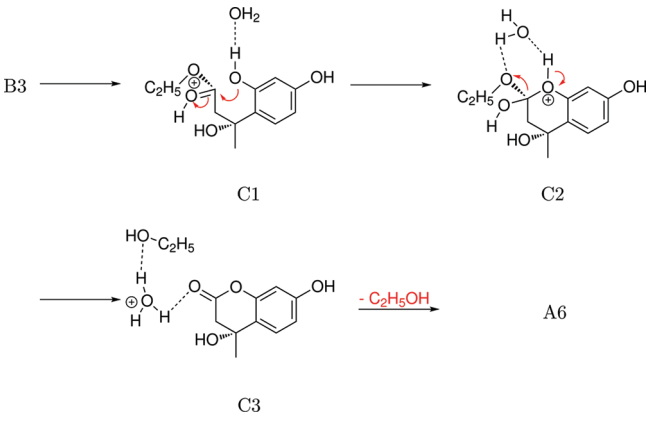

Figure 8. Reaction scheme of the "C" mechanism.

Turning to the individual profiles first we start with the discussion of route A. As Figure 6 shows the first step here is the trans-esterification. The β-keto-ester intermediate (A3) resulted from this steps can be identified as expectedly the longest-lived intermediate, owing to the high (∼14 kcal/mol) activation energies in either direction. This prediction is in accordance with the experimental observations supporting the mechanism by Ahmed et al. Proceeding along the reaction path the next step is the electrophilic attack on the aromatic ring and the C−C bond formation. At this step the system goes through the highest point of the free energy profile (27.0 kcal/mol). Reaching the A5 stage yields substantial energy by restoring the aromaticity. A couple of proton scramblings and water elimination lead to the final product, protonated coumarin. The last step is highly exergonic, due to the formation of the extended electron delocalization in A8.

The reaction scheme for the B mechanism can be seen in Figure 7. The initial step of this path is the electrophilic attack of ethyl acetoacetate to resorcinol leading to B2. After its deprotonation, the relatively stable B3 intermediate is formed by passing the highest free energy state of the profile (30.0 kcal/mol). As the subsequent step requires quite high activation free energy (11.5 kcal/mol), this intermediate may have a lifetime long enough to be observed. The following steps are water elimination and fast proton migrations yielding B6. Its relatively high stability implies that along route B this intermediate can be another long-lived species. In fact, within the free energy well-defined by the B3 and B6, the intermediates can rearrange into each other in the presence of water. These intermediates are structurally related to cinnamic acid, which is an important side product of the Pechmann condensation.[12] This implies that the calculated free energy profile for route B is in accord with the experimental proposal of Robertson et al. We also note that B6 is the compound recently identified by GC-MS among the side products

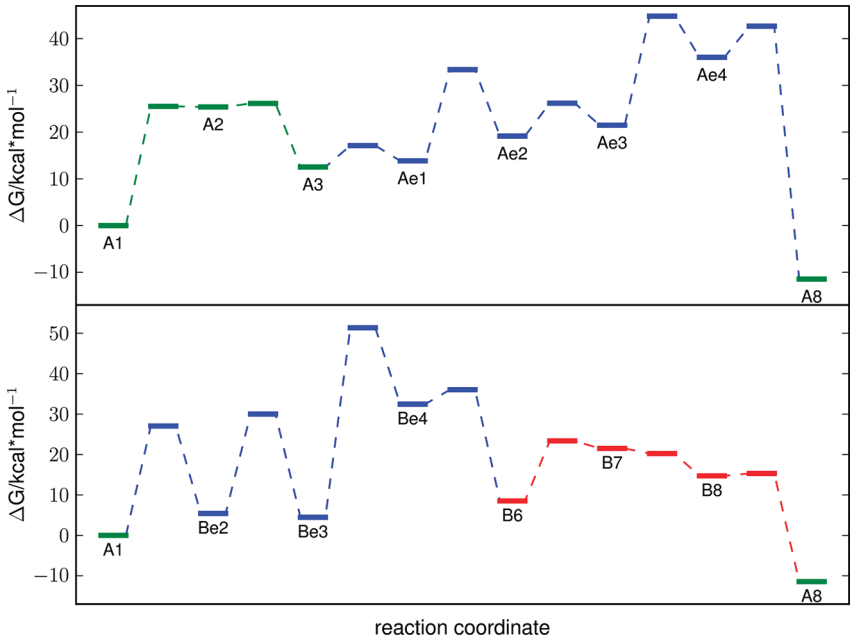

Figure 9. Gibbs free energy diagram for A_e mechanism (upper panel) and B_e mechanism (lower panel).

dx.doi.org/10.1021/jo201439u |J. Org. Chem. 2011, 76, 8749–8755

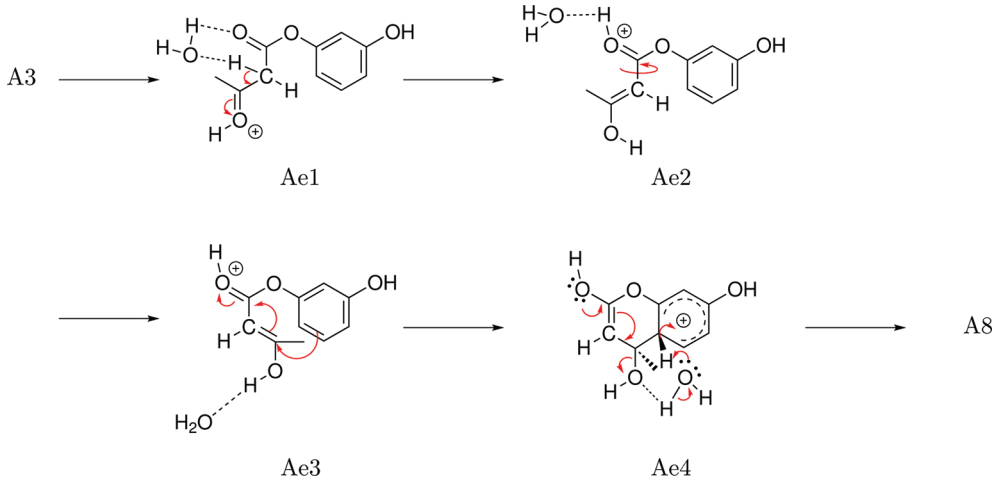

Figure 10. Reaction scheme of the A_e mechanism.

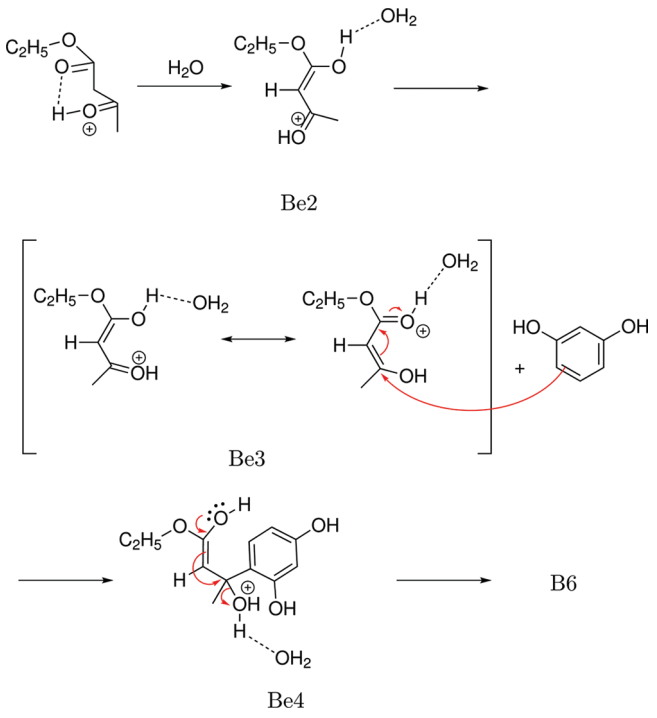

Figure 11. Reaction scheme of the B_e mechanism.

of the Pechmann reaction.[22] In a substantially endergonic step, B6 rearranges to B7 featuring already the coumarin skeleton. The high energy investment is required by the formation of the unstable orthoester group, which subsequently transforms to the product by losing an ethanol molecule.

Route C follows route B until B3, then C diverges from path B and reaches path A (Figure 8). Along route C, intermediate B3 undergoes trans-esterification by closing the lactone ring. In the subsequent steps, proton migrations and the ethyl alcohol dissociation take place and then route C combines with route A at stage A6. The most stable intermediate of this path is predicted to be B3 again. The highest transition state level with respect to the reactants' level is 30.0 kcal/mol, connecting B3 and C1 intermediates. After this stage, route C features an overall downhill free energy profile. It follows therefore that the B and C routes cannot be distinguished on the basis of their kinetics.

Comparison of the three possible routes shows that the overall free energy barriers are very similar for each mechanism. In fact, they agree within the margin of error of the methodology. Hence, we conclude that the three routes can operate simultaneously and additional experimental factors could determine the dominant path. All three calculated routes can account for the experimentally observed intermediates and side-products by predicting them to be relatively stable on the reaction free energy surfaces.

3.2. Enolic Routes. To decide whether the enolic or oxo form of the β-keto-ester moiety can perform the electrophilic attack in an energetically more favorable way, we have also computed the free energy profiles for the possible enolic routes. Figure 9 displays the calculated free energy curves for mechanisms A and B with enol tautomers. Since route C is identical with route B at the electrophilic attack stage, there are only two possible enolic routes.

The enol alternative of path A is shown in Figure 10. Along this path, intermediate A3, after a conformational change, enolizes to Ae2. This solvent-assisted tautomerism requires high, 19.4 kcal/mol activation energy. The electrophilic attack is preceded by an additional conformational change (Ae3). Note the positive charge on the ester group which was essential to stabilize the intermediate. The C−C bond formation via the enolic form (Ae3−Ae4) requires again high activation free energy (~23 kcal/mol). Overall, this route requires 45.4 kcal/mol activation free energy. On the basis of the very high barrier, this route can be excluded.

Figure 11 shows the enol version of mechanism B (B_e). Along this path the enolization takes place at the reactant stage with quite high, *ca.* 30 kcal/mol activation energy. After a conformational change, the electrophilic attack occurs with extremely high activation energy (48 kcal/mol). The overall free energy barrier is even higher, more than 50 kcal/mol. Clearly, this process is again highly unfavorable; hence, we can discard this mechanism as well.

4. CONCLUSIONS

We have performed density functional calculations to calculate the reaction free energy profiles for various possible routes for the Pechmann condensation. We have obtained that the three possible oxo routes can operate simultaneously. In contrast, the

dx.doi.org/10.1021/jo201439u |*J. Org. Chem.* 2011, 76, 8749–8755

mechanisms suggesting that the electrophilic attack can occur via the enol tautomer of the β-keto-ester moiety could be excluded on the basis of their very high free energy barriers. Stable reaction intermediates have been identified on the free energy profiles for the oxo routes, namely β-keto-ester intermediate on route A and cinnamic-acid derivatives along B and C routes. They can explain experimental observations and can assist in further experimental characterizations of the Pechmann-type reactions.

■ ASSOCIATED CONTENT

Supporting Information. Cartesian coordinates, computed total energies, Gibbs free energies and where applicable the value of the imaginary frequencies of the optimized structures are collected. This material is available free of charge via the Internet at http://pubs.acs.org.

■ AUTHOR INFORMATION

Corresponding Author
*stirling@chemres.hu

■ ACKNOWLEDGMENT

We acknowledge fruitful discussions with Tibor Soós. This work has been supported by OTKA Grant K-68360.

■ REFERENCES

(1) O'Kennedy, R.; Thornes, R. *Coumarins: biology, applications, and mode of action*; John Wiley & Sons: New York, 1997.
(2) Lacy, A.; O'Kennedy, R. *Cur. Pharm. Des.* **2004**, *10*, 3797–3811.
(3) Borges, F.; Roleira, F.; Milhazes, N.; Santana, L.; Uriarte, E. *Cur. Med. Chem.* **2005**, *12*, 887–916.
(4) Trenor, S. R.; Shultz, A. R.; Love, B. J.; Long, T. E. *Chem. Rev.* **2004**, *104*, 3059–3078.
(5) Riveiro, M. E.; De Kimpe, N.; Moglioni, A.; Vazquez, R.; Monczor, F.; Shayo, C.; Davio, C. *Curr. Med. Chem.* **2010**, *17*, 1325–1338.
(6) For further medicinal and biological applications of coumarins see: (a) Hoult, J. R. S.; Payá, M. *Gen. Pharmacol.* **1996**, *27*, 713–22. (b) Fylaktakidou, K. C.; Hadjipavlou-Litina, D. J.; Litinas, K. E.; Nicolaides, D. E. *Curr. Pharm. Des.* **2004**, *10*, 3813–3833. (c) Rappl, C.; Barbier, P.; Bourgarel-Rey, V.; Gregoire, C.; Gilli, R.; Carre, M.; Combes, S.; Finet, J.-P.; Peyrot, V. *Biochemistry* **2006**, *45*, 9210–9218. (d) Curini, M.; Cravotto, G.; Epifano, F.; Giannonei, G. *Curr. Med. Chem.* **2006**, *13*, 199–222. (e) Menasria, F.; Azebaze, A. G. B.; Billard, C.; Faussat, A. M.; Nkengfack, A. E.; Meyer, M.; Kolb, J. P. *Leuk. Res.* **2008**, *32*, 1914–1926. (f) Zhao, H.; Donnelly, A. C.; Kusuma, B. R.; Brandt, G. L. E.; Brown, D.; Rajewski, R. A.; Vielhauer, G.; Holzbeierlein, J.; Cohen, M. S.; Blagg, B. S. J. *J. Med. Chem.* **2011**, *54*, 3839–3853. (g) Benigni, R.; Bossa, C. *Chem. Rev.* **2011**, *111*, 2507–2536 and references therein.
(7) Lake, B. G. *Food Chem. Toxicol.* **1999**, *37*, 423–453.
(8) Joshi, R.; Chudasama, U. *J. Sci. Ind. Res.* **2008**, *67*, 1092–1097.
(9) v. Pechmann, H. *Berichte der deutschen chemischen Gesellschaft* **1884**, *17*, 929.
(10) Srinivasan, P.; Rao, V. J.; Chandrasekaran, S.; Rampally, C. Process for preparing substituted coumarins; US Patent No. 6716996 B1, 2004.
(11) Flavin, M. T.; Xu, Z.-Q.; Khilevich, A.; Zembower, J. D.; Liao, S.; Mar, A.; Lin, V.; Brankovic, D.; Dzekhster, S.; Liu, J. Method for the preparation of (+)-calanolide A and analogues thereof; US Patent No. 5,977,385, 1998.
(12) Sethna, S. M.; Shah, N. M. *Chem. Rev.* **1945**, *36*, 1–62.
(13) Maheswara, M.; Siddaiah, V.; Damu, G. L. V.; Rao, Y. K.; Rao, C. V. *J. Mol. Catal. A* **2006**, *255*, 49–52.
(14) Woods, L. L.; Sapp, J. A *J. Org. Chem.* **1962**, *27*, 3703–3705.
(15) Shirini, F.; Marjani, K.; Nahzomi, H. T.; Zolfigol, M. A. *Chin. Chem. Lett.* **2007**, *18*, 909–911.
(16) Kokare, N. D.; Sangshetti, J. N.; Shinde, D. B. *Chin. Chem. Lett.* **2007**, *18*, 1309–1312.
(17) Torviso, R.; Mansilla, D.; Belizán, A.; Alesso, E.; Moltrasio, G.; Vázquez, P.; Pizzio, L.; Blanco, M.; Cres, C. *Appl. Catal., A* **2008**, *339*, 53–60.
(18) Dong, F.; Jian, C.; Kai, G.; Qunrong, S.; Zuliang, L. *Catal. Lett.* **2008**, *121*, 255–259.
(19) John, E.; Israelstam, S. *J. Org. Chem.* **1961**, *26*, 240–242.
(20) Bose, D. S.; Rudradas, A.; Babu, M. H. *Tetrahedron Lett.* **2002**, *43*, 9195–9197.
(21) Robertson, A.; Waters, R. B.; Jones, E. T. *J. Chem. Soc.* **1932**, 1681–1688.
(22) Tyagi, B.; Mishra, M. K.; Jasra, R. V. *J. Mol. Catal. A* **2007**, *276*, 47–56.
(23) Calvino-Casilda, V.; Banares, M.; LozanoDiz, E. *Catal. Today* **2010**, *155*, 279–281.
(24) Guo, X.; Yu, R.; Li, H.; Li, Z. *J. Am. Chem. Soc.* **2009**, *131*, 17387–17393.
(25) Sinhamahapatra, A.; Sutradhar, N.; Pahari, S.; Bajaj, H. C.; Panda, A. B. *App. Catal. A* **2011**, *394*, 93–100.
(26) Frisch, M. J.; Trucks, G. W.; Schlegel, H. B.; Scuseria, G. E.; Robb, M. A.; Cheeseman, J. R.; Scalmani, G.; Barone, V.; Mennucci, B.; Petersson, G. A.; Nakatsuji, H.; Caricato, M.; Li, X.; Hratchian, H. P.; Izmaylov, A. F. et al. *Gaussian 09*, Revision A.02; Gaussian Inc.: Wallingford, CT, 2009.
(27) Zhao, Y.; Schultz, N. E.; Truhlar, D. G. *J. Chem. Theor. Comp.* **2006**, *2*, 364–382.
(28) Marenich, A. V.; Cramer, C. J.; Truhlar, D. G. *J. Phys. Chem. B.* **2009**, *113*, 6378–6396.
(29) Jensen, F. *Introduction to Computational Chemistry*; John Wiley & Sons: New York, 2006.
(30) Gutiez-Shez, C.; Calvino-Casilda, V.; Pz-Mayoral, E.; MartAranda, R.; L-Peinado, A.; Bejblova, M.; Cejka, J. *Catal. Lett.* **2009**, *128*, 318–322.
(31) (a) Tomasi, J.; Mennucci, B.; Cammi, R. *Chem. Rev.* **2005**, *105*, 2999–3093. (b) Kelly, C. P.; Cramer, C. J.; Truhlar, D. G. *J. Phys. Chem. A* **2006**, *110*, 2493–2499. (c) Wang, X.; Fu., H.; Du, D.; Zhou, Z.; Zhang, A.; Su, C.; Ma, K. *Chem. Phys. Lett.* **2008**, *460*, 339–342. (d) Bryantsev, V. S.; Diallo, M. S.; Goddard, W. *J. Phys. Chem. B* **2008**, *112*, 9709–9719. (e) Stanković, S.; Catak, S.; D'hooghe, M.; Goossens, H.; Abbaspour Tehrani, K.; Bogaert, P.; Waroquier, M.; Van Speybroeck, V.; De Kimpe, N. *J. Org. Chem.* **2011**, *76*, 2157–2167. (f) Siegbahn, P. E. M. *J. Phys. Chem.* **1996**, *100*, 14672–14680.